

# Phase-preserving amplitude regeneration in a Mamyshev regenerator with mid-stage optical phase conjugation

Cheng Guo and Michael Vasilyev\*

*Department of Electrical Engineering, University of Texas at Arlington, Arlington, TX, USA*

\*[vasilyev@uta.edu](mailto:vasilyev@uta.edu)

**Abstract:** We experimentally demonstrate phase-preserving amplitude regeneration of an RZ-QPSK signal by placing an optical phase conjugator between two Mamyshev regenerators, improving intensity noise 2.8 times, Q-factor by 2.4 dB and EVM by 4.0%. © 2022 The Authors

## 1. Introduction

All-optical regenerators can potentially offer dramatic savings of cost, space, and power consumption, compared to their optoelectronic counterparts [1]. The Mamyshev regenerator [2], based on self-phase-modulation- (SPM)-caused spectral broadening followed by off-center filtering, is arguably the most robust and effective all-optical scheme providing amplitude 2R regeneration (re-amplification + re-shaping). Most importantly, it can be modified to simultaneously process any number of wavelength-division multiplexing (WDM) channels, if a conventional highly nonlinear fiber (HNLF) in it is replaced by a group-delay-managed (GDM) nonlinear medium [3]. Unfortunately, while Mamyshev regenerator works well with on-off-keying (OOK) modulation format, it is not compatible with the advanced modulation formats carrying any part of information in the signal phase (e.g., phase-shift keying, or PSK, and quadrature amplitude modulation, or QAM), because strong SPM in the regenerator results in significant amplitude-to-phase noise transfer, destroying the phase information. There are alternative schemes that offer amplitude regeneration without disturbing the phase, which are known as phase-preserving amplitude regenerators (PPARs). In most practical scenarios the amplitude regeneration of phase-encoded signals is sufficient, because it prevents nonlinear amplitude-to-phase noise conversion in the subsequent transmission links, hereby eliminating the most dominant source of phase noise and making the phase regeneration (which typically requires the use of phase-sensitive amplifiers [4]) unnecessary. A popular PPAR based on a nonlinear-optical loop mirror (NOLM) has been demonstrated with PSK [5], star8-QAM [6] and 8-PSK [7] formats. The interferometric nature of the NOLM-based PPAR, however, makes it significantly less robust than Mamyshev scheme, and strong Rayleigh backscattering noise prevents NOLM's use with GDM nonlinear medium, thus limiting its operation to just a single WDM channel.

In this paper, we experimentally demonstrate how to turn Mamyshev regenerator into a PPAR, preserving its robustness and potential for multi-channel operation, while eliminating the nonlinear amplitude-to-phase noise conversion. For that, we split the Mamyshev regenerator into two regenerating stages with an optical phase conjugator (OPC) placed between them. Mid-link OPC has been shown to reverse nonlinear evolution in transmission links (see, e.g., [8]), in which any nonlinearity is seen as a nuisance. In our work, under proper operating conditions, the amplitude-to-phase noise conversion in the first Mamyshev regeneration stage (MR1) is reversed after the OPC by the second Mamyshev stage (MR2), while the SPM-induced amplitude regeneration remains irreversible ("locked-in" by the optical bandpass filter).

## 2. Experimental setup

Our experimental setup is shown in Fig. 1(a). 10-Gbaud NRZ-QPSK-modulated signal is generated by an IQ coherent transmitter (IQTX-26-EDP-ABC-C, Quantifi Photonics) driven by an arbitrary waveform generator (Agilent M8195A) with root-raised-cosine (RRC) filter with a roll-off factor of 0.7 at wavelength of 1562.23 nm (ITU channel 19). The modulated signal is carved into 50% RZ pulses by an intensity modulator driven by the symbol-rate clock. After that, the signal is loaded with amplitude noise by another intensity modulator driven by amplified Nyquist-Johnson thermal noise with 14 GHz bandwidth. This noise is generated by 8 cascaded RF amplifiers. All constellation map measurements are done by LeCroy optical modulation analyzer (OMA, LabMaster 10-65Zi-A with IQS70 coherent receiver) with signal pre-amplified to 16 dBm by an erbium-doped fiber amplifier (EDFA) before the OMA.

The generated noisy 50% RZ-QPSK signal is sent to the MR1 [red-dash-bordered block in Fig 1(a)] for partial regeneration of the amplitude. In MR1 the signal is amplified by an EDFA, passed through 150-GHz-wide optical bandpass filter (OBPF) to remove out-of-band amplified spontaneous emission (ASE) noise, and sent into 8.8-km-long SMF-LS™ fiber at an average power level of 16.7 dBm to accumulate a peak nonlinear phase shift of 1.15 rad. SMF-LS™ is a non-zero dispersion-shifted fiber with slightly normal dispersion (−0.5...−3.0 ps/nm/km) in the C-band. Then the signal is filtered by two cascaded 0.25-nm-wide OBPFs to achieve a moderate amount of amplitude regeneration. Since QPSK format does not have any symbols with zero amplitude level, the OBPFs do not need to be off-centered. The spectra of the input noisy signal at the location **A** in Fig. 1(a) and the SPM-broadened (or partially

regenerated) signal at the location **B'** (or **B**) are shown in the top graph of Fig. 1(b) by the red and green curves, respectively. The constellation maps, as well as intensity and phase histograms corresponding to locations **A** and **B** are shown in the first two columns of Fig. 2. The standard deviation of the intensity distribution shrinks from  $\sigma \approx 0.30$  before MR1 to  $\sigma \approx 0.19$  after MR1, demonstrating (at least partial) amplitude regeneration by MR1. However, the signal's phase undergoes significant distortion due to nonlinear amplitude-to-phase noise transfer, as is clearly visible in both the constellation map and phase histogram after MR1.

After MR1 the signal is sent to the fiber-parametric-amplifier-based OPC [green-dash-bordered block in Fig 1(a)]. The OPC pump at wavelength of 1552.54 nm (ITU channel 31) is generated by Ando AQ4321A tunable laser source (TLS) and is amplified by an EDFA. The amplified pump is filtered by two OBPFs (0.8 nm and 1 nm bandwidths) to remove the out-of-band ASE noise. The clean pump is sent into the OPC through port 1 of a circulator that is used to redirect back-propagating stimulated Brillouin scattering (SBS) light into an optical trap at port 3. From port 2 of the circulator, the pump is sent to a polarization controller (PC) used to align the polarization states of the pump and the signal and is combined by a WDM coupler with the signal. Then the signal and pump enter a 500-m-long dispersion-flattened highly nonlinear fiber (DF-HNLF) with  $\gamma = 21.4/\text{W}/\text{km}$  and zero-dispersion wavelength of 1551.5 nm. The input power of the signal is kept at  $-1$  dBm to avoid nonlinear phase shift accumulation in DF-HNLF. The output idler is generated at 1542.94 nm (ITU channel 43) with  $-17$ -dBm power, which represents conversion efficiency (CE) of  $-16$  dB. The low CE is due to the SBS threshold that limits the continuous-wave (CW) pump power to 16.2 dBm [9]. The idler is filtered by a 150-GHz-wide OBPF and sent to MR2 [blue-dash-bordered block in Fig 1(a)]. The spectrum of filtered idler at the location **C** in Fig. 1(a) is shown with blue curve in the bottom graph of Fig. 1(b). The corresponding constellation map, as well as intensity and phase histograms are shown in the 3<sup>rd</sup> column of Fig. 2. The idler beam's intensity distribution has standard deviation  $\sigma \approx 0.22$ , representing small increase compared to the signal entering the OPC, owing to poor idler noise figure at low CE and, possibly, some relative-intensity noise transfer from pump to idler. The constellation maps indicate that the nonlinear phase distortion map of the signal is flipped vertically after the OPC, as expected, while the amount of phase distortion remains approximately the same (standard deviation of phase  $\approx 15.4^\circ$ ).

In MR2, the filtered idler is amplified by two cascaded EDFAs to 19.8 dBm and sent through a 5.1-km-long SMF-LS<sup>TM</sup> to accumulate a peak nonlinear phase shift of 1.46 rad. Then, the idler is filtered by a 20-GHz-wide OBPF to realize the amplitude regeneration. The SPM-broadened idler at location **D'** and regenerated idler at the location **D** in Fig. 1(a) are shown with dashed and solid purple curves, respectively, in the bottom graph of Fig. 1(b). The constellation map, as well as intensity and phase histograms corresponding to **D** are shown in the 4<sup>th</sup> column of Fig. 2. The regenerated idler beam has standard deviation of the intensity distribution  $\sigma = 0.106$ , representing 2.8-times reduction compared to the intensity noise at the input of MR1. The constellation map and phase histogram of the output idler beam indicate that the nonlinear phase distortion introduced by MR1 is mostly compensated (its standard deviation is reduced from  $\approx 15.8^\circ$  to  $\approx 7^\circ$ , which is just a small increase over input  $5.1^\circ$  deviation), and the EVM and Q-factor improvements over the MR1 input are 4.0% and 2.4 dB, respectively. The amplitude noise suppression by this 3-stage regenerator can significantly reduce the nonlinear amplitude-to-phase noise transfer in any subsequent nonlinear propagation through transmission fibers, leading to potential reach increase.

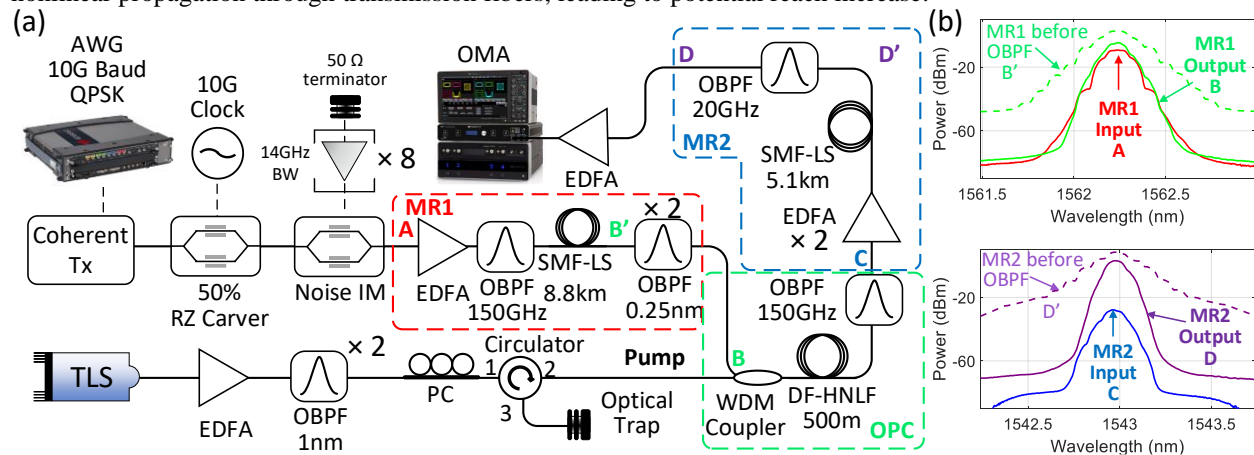


Fig. 1. (a) Experimental setup for amplitude-noise-degraded signal preparation, 3-stage phase-preserving amplitude regeneration, and coherent system characterization. AWG: Arbitrary waveform generator; BW: bandwidth; DF-HNLF: dispersion-flattened highly-nonlinear fiber; EDFA: erbium-doped fiber amplifier; IM: Intensity modulator; OBPF: optical bandpass filter; PC: Polarization controller; RZ: return-to-zero; Tx: transmitter; WDM: wavelength division multiplexing. (b) Spectra at locations **A** (solid red), **B** (solid green), **B'** (dashed green), **C** (solid blue), **D** (solid purple), and **D'** (dashed purple) in (a).

### 3. Summary

We have demonstrated phase-preserving amplitude regeneration of a 10-Gbaud 50%-duty-cycle RZ-QPSK signal by a 3-stage optical regenerator combining two Mamyshev regenerators and an optical phase conjugator placed between them. The regeneration improves Q-factor by 2.4 dB, EVM by 4.0%, and reduces the standard deviation of the intensity by 2.8 times. Since both Mamyshev regenerator and optical phase conjugator are potentially compatible with multi-channel operation, this work paves the way for future multi-channel phase-preserving regeneration of advanced modulation formats.

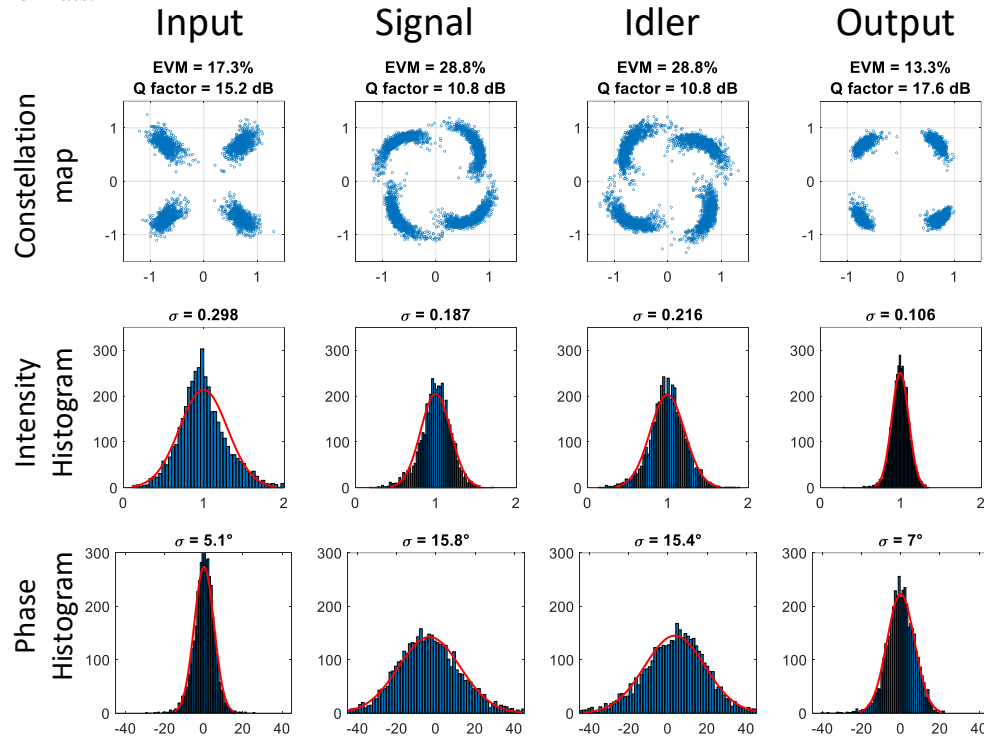


Fig. 2. Constellation maps (1<sup>st</sup> row), intensity histograms (2<sup>nd</sup> row) and phase histogram (3<sup>rd</sup> row) for: (1<sup>st</sup> column) regenerator input at location **A** in Fig. 1(a), (2<sup>nd</sup> column) first-stage output at location **B**, (3<sup>rd</sup> column) idler at the OPC output at location **C**, and (4<sup>th</sup> column) regenerator output at location **D**. Red lines in the 2<sup>nd</sup> and 3<sup>rd</sup> rows show Gaussian fits.

### 4. Acknowledgement

We thank Y. Akasaka and P. Palacharla of Fujitsu Network Communications for useful discussions about SBS and S. Takasaka and R. Sugizaki of Furukawa Electric Co., Ltd. for providing us with dispersion-flattened HNLF.

### 5. References

- [1] P. G. Patki, P. Guan, L. Li, T. I. Lakoba, L. K. Oxenløwe, M. Vasilyev, and M. Galili, "Recent Progress on Optical Regeneration of Wavelength-Division-Multiplexed Data," *J. Sel. Top. Quant. Electron.* **27**, 7700812 (2021).
- [2] P. V. Mamyshev, "All-optical data regeneration based on self-phase modulation effect," in *Proc. of the European Conference on Optical Communications (ECOC)*, Madrid, Spain, 1998, pp. 475–476.
- [3] L. Li, P. G. Patki, Y. B. Kwon, V. Stelmakh, B. D. Campbell, M. Annamalai, T. I. Lakoba, and M. Vasilyev, "All-optical regenerator of multi-channel signals," *Nature Comm.* **8**, 884 (2017).
- [4] R. Slavík, F. Parmigiani, J. Kakande, C. Lundström, M. Sjödin, P. A. Andrekson, R. Weerasuriya, S. Sygletos, A. D. Ellis, L. Grüner-Nielsen, D. Jakobsen, S. Herstrøm, R. Phelan, J. O'Gorman, A. Bogris, D. Syvridis, S. Dasgupta, P. Petropoulos, and D. J. Richardson, "All-optical phase and amplitude regenerator for next-generation telecommunications systems," *Nature Photon.* **4**, 690 (2010).
- [5] K. Cvecek, K. Sponsel, C. Stephan, G. Onishchukov, R. Ludwig, C. Schubert, B. Schmauss, and G. Leuchs, "Phase-preserving amplitude regeneration for a WDM RZ-DPSK signal using a nonlinear amplifying loop mirror," *Opt. Express* **16**, 1923 (2008).
- [6] T. Roeslingshoefer, T. Richter, C. Schubert, G. Onishchukov, B. Schmauss, and G. Leuchs, "All-optical phase-preserving multilevel amplitude regeneration," *Opt. Express* **22**, 27077 (2014).
- [7] C. Guo, M. Vasilyev, and T. I. Lakoba, "Amplitude regeneration and phase noise suppression of an 8-PSK signal by an attenuation-imbalanced NOLM," *CLEO 2022 conference*, San Jose, CA, May 15–20, 2022, paper STh5M.6.
- [8] K. Solis-Trapala, T. Inoue, and S. Namiki, "Nearly-ideal optical phase conjugation based nonlinear compensation system," *Optical Fiber Communication (OFC) conference*, San Francisco, CA, March 9–13, 2014, paper W3F.8.
- [9] C. Guo, M. Vasilyev, Y. Akasaka, and P. Palacharla, "Alignment of zero-dispersion wavelength along highly-nonlinear fiber length with simultaneous increase in the stimulated Brillouin scattering threshold," *Optical Fiber Communication (OFC) conference*, San Diego, CA, March 6–10, 2022, paper W3E.2.